



Published in final edited form as:

Cancer Res. 2007 June 1; 67(11): 5425–5433. doi:10.1158/0008-5472.CAN-06-4431.

Mapping Genes that Contribute to Daunorubicin-Induced Cytotoxicity

Shiwei Duan¹, Wasim K. Bleibel¹, Rong Stephanie Huang¹, Sunita J. Shukla², Xiaolin Wu¹, Judith A. Badner³, and M. Eileen Dolan¹

¹Department of Medicine, The University of Chicago, Chicago, Illinois

²Department of Human Genetics, The University of Chicago, Chicago, Illinois

³Department of Psychiatry, The University of Chicago, Chicago, Illinois

Abstract

Daunorubicin is an anthracycline antibiotic agent used in the treatment of hematopoietic malignancies. Toxicities associated with this agent include myelosuppression and cardiotoxicity; however, the genes or genetic determinants that contribute to these toxicities are unknown. We present an unbiased genome-wide approach that incorporates heritability, whole-genome linkage analysis, and linkage-directed association to uncover genetic variants contributing to the sensitivity to daunorubicin-induced cytotoxicity. Cell growth inhibition in 324 Centre d' Etude du Polymorphisme Humain lymphoblastoid cell lines (24 pedigrees) was evaluated following treatment with daunorubicin for 72 h. Heritability analysis showed a significant genetic component contributing to the cytotoxic phenotypes ($h^2 = 0.18-0.63$ at 0.0125, 0.025, 0.05, 0.1, 0.2, and 1.0 $\mu\text{mol/L}$ daunorubicin and at the IC_{50} , the dose required to inhibit 50% cell growth). Whole-genome linkage scans at all drug concentrations and IC_{50} uncovered 11 regions with moderate peak LOD scores (>1.5), including 4q28.2 to 4q32.3 with a maximum LOD score of 3.18. The quantitative transmission disequilibrium tests were done using 31,312 high-frequency single-nucleotide polymorphisms (SNP) located in the 1 LOD confidence interval of these 11 regions. Thirty genes were identified as significantly associated with daunorubicin-induced cytotoxicity ($P \leq 2.0 \times 10^{-4}$, false discovery rate ≤ 0.1). Pathway and functional gene ontology analysis showed that these genes were overrepresented in the phosphatidylinositol signaling system, axon guidance pathway, and GPI-anchored proteins family. Our findings suggest that a proportion of susceptibility to daunorubicin-induced cytotoxicity may be controlled by genetic determinants and that analysis using linkage-directed association studies with dense SNP markers can be used to identify the genetic variants contributing to cytotoxicity.

Introduction

Daunorubicin is a chemotherapeutic agent used in the treatment of hematopoietic malignancies, such as acute lymphocytic and acute myelogenous leukemia, as well as some lymphomas and breast cancer (1). There are several proposed mechanisms of daunorubicin, most notably DNA intercalation, with a preference for dGdC-rich regions flanked by A/T basepairs (2). Daunorubicin has also been shown to inhibit DNA topoisomerase II by trapping DNA strand

©2007 American Association for Cancer Research.

Requests for reprints: M. Eileen Dolan, Department of Medicine, University of Chicago, 5841 S. Maryland Avenue, Box MC2115, Chicago, IL 60637. Phone: 773-702-4441; Fax: 773-702-0963; E-mail: edolan@medicine.bsd.uchicago.edu.

Note: Supplementary data for this article are available at Cancer Research Online (<http://cancerres.aacrjournals.org/>)

A Pharmacogenetics of Anticancer Agents Research Group study (<http://pharmacogenetics.org>).

passage intermediates, eventually resulting in DNA single-strand and double-strand breaks. Recent studies have shown that the formation of DNA-anthracycline complexes can significantly modify the ability of the helicases to separate DNA into single strands in an ATP-dependent fashion, thereby hindering the process of strand separation and limiting replication (3). There are also reports that this drug can inhibit protein kinase C pathways (4). Patients often initially respond but then relapse due to resistance mechanisms, such as P-170 glycoprotein-mediated drug efflux, altered topoisomerase II activity, or overexpression of bcl-2 (5).

The cumulative and dose-dependent toxicities that have limited the usage of daunorubicin are myelosuppression, mucositis, and cardiotoxicity (6–8). The risk of anthracycline-induced cardiotoxicity is 10% to 26% and is dependent primarily on dose (9,10). Anthracycline-induced cardiotoxicity is thought to be mediated through reactive oxygen species production. Experiments conducted on rat cardiomyocytes have shown that corticosterone can inhibit apoptosis induced by doxorubicin, a structural analogue of daunorubicin. This effect was mediated by the regulation of multiple genes, including antioxidant/detoxification enzymes, receptors, signaling molecules, and amino acid and protein synthesis (11). Furthermore, Yi et al. have identified significant gene expression changes in mice after doxorubicin treatment, including a series of genes that encode oxidative stress-related proteins, signal transduction, and apoptotic proteins (12). Matrix metalloproteinases 2 and 9 expression levels were enhanced in mice after acute doxorubicin treatment (13). In humans, tumor necrosis factor α and phospholipase C- δ 1 have been shown to be critical in doxorubicin-induced cardiotoxicity (14). The genes important in daunorubicin-induced cardiotoxicity have not been well studied.

In this report, we used classic and modern genetic approaches to identify genes that contribute to daunorubicin-induced cytotoxicity. To this end, lymphoblastoid cell lines (LCLs) derived from large Centre d' Etude du Polymorphisme Humain (CEPH) pedigrees of Northern and Western European descent were used to identify the extent to which heritable factors contribute to drug cytotoxicity. There have been candidate gene approaches to study the cellular sensitivity of daunorubicin in multiple tumor cell lines (15–19). However, our approach uses whole-genome linkage analysis and linkage-directed association studies to facilitate identifying regions within the genome that harbor genes contributing to daunorubicin-induced cytotoxicity.

Materials and Methods

Cell lines

LCLs derived from 24 Caucasian Utah CEPH families (1331, 1333, 1334, 1340, 1341, 1344, 1345, 1346, 1347, 1349, 1350, 1358, 1362, 1375, 1408, 1413, 1416, 1420, 1423, 1444, 1447, 1454, 1459, and 1463) were purchased from the Coriell Institute for Medical Research⁴ (Camden, NJ). Cell lines were maintained in RPMI 1640 (Mediatech) supplemented with 15% fetal bovine serum (HyClone) and 1% L-glutamine (Invitrogen). Cell lines were passaged thrice per week at a concentration of 350,000 cells/mL and kept at a temperature of 37°C, with 5% CO₂ and 95% humidity.

Drug

Daunorubicin (NSC-82151) was kindly provided by the Drug Synthesis and Chemistry Branch, Division of Cancer Treatment, National Cancer Institute (NCI), Bethesda, MD.

⁴Coriell Institute for Medical Research; <http://www.locus.umdj.edu/ccr/>.

Cell cytotoxicity assay

Cell growth inhibition was evaluated at concentrations of 0, 0.0125, 0.025, 0.05, 0.1, 0.2, and 1.0 $\mu\text{mol/L}$ daunorubicin. These concentrations were selected through assay optimization over a large range of daunorubicin treatment concentrations. We chose the daunorubicin concentrations within the limits of our assay that best characterized the sigmoid shape of cell growth inhibition. Daunorubicin was prepared in PBS (pH 7.4; Invitrogen) immediately before use. The cytotoxic effect of daunorubicin on these CEPH cell lines was determined using the nontoxic colorimetric-based assay, AlamarBlue (Biosource). Cell viability was assessed on exponentially growing LCLs by trypan blue dye exclusion using the Vi-Cell XR viability analyzer (Beckman Coulter). Cells (100 μL) with viabilities of >85% were plated at a density of 1×10^5 cells/mL (1×10^4 cells per well), in triplicate, in 96-well round-bottomed plates (Corning). After 24 h incubation, cells were treated with either vehicle (media contains 0.1% PBS) or increasing concentrations of daunorubicin for 72 h. At 72-h incubation time, untreated cells were in exponential growth. AlamarBlue was added 24 h before absorbance reading at wavelengths 570 and 600 nm using the Synergy-HT multidetection plate reader (BioTek). Percentage survival was quantified using manufacturer's protocol.⁵ Final percentage survival was averaged from at least six replicates from two independent experiments. Additionally, the drug concentration required to inhibit 50% of cell growth (IC_{50}) was determined for each cell line. Unsupervised, global hierarchical clustering was done on the daunorubicin cytotoxic phenotypes with percentage survival data for each cell line using the complete linkage method, as implemented in the Partek Genomics Solution software (Partek Inc.).

Heritability analysis

Heritability analysis was done using Sequential Oligogenic Linkage Analysis Routines (SOLAR)⁶ to estimate narrow sense heritability (h^2) and test its significance at each treatment concentration. This analysis allowed us to quantify the proportion of inherited factors contributing to human LCL variation in sensitivity to daunorubicin. SOLAR uses likelihood ratio tests to evaluate heritability by comparing a purely polygenic model with a sporadic model in the case of testing heritability (20). All phenotype data were transformed using the inverse normalization of the percentile rank function in Microsoft Excel software. Covariates, such as age, sex, and age \times sex interaction, were tested in the heritability model. Sex-specific heritability was also analyzed by setting the phenotypes for one gender to unknown and analyzing the heritability for the other gender. The significance of differences in male and female heritability was assessed through randomly permuting male and female genders, keeping the numbers of males and females within a pedigree constant, and performing the sex-specific heritability analysis in each replicate.

Error checking

Error checking for Mendelian incompatibility, misspecified relationships, and unlikely recombinations has been done as described previously (21); however, this study used a much denser map. The web-based platform integrates and formats data (pedigree, genotype, phenotype) and executes error checking using PedCheck (22) to detect genotypic incompatibilities, PREST (23) to detect relationship misspecifications and multipoint engine for rapid likelihood inference (MERLIN)⁷ (24) to detect unlikely recombinants before linkage analysis and is enabled to run linkage analysis on multiple platforms including MERLIN, GENE-HUNTER, and SOLAR. From the combined pool of genotyped markers, 7,209 single-nucleotide polymorphisms (SNPs) and microsatellite nonredundant markers yielding a very

⁵Cell percentage survival calculation; <http://www.invitrogen.com/content/sfs/manuals/BioSource%20DAL1100.pdf>.

⁶SOLAR; <http://www.sfbr.org/solar/>.

⁷MERLIN; <http://www.sph.umich.edu/csg/abecasis/Merlin/>.

dense genetic map with highly heterozygous markers (heterozygosity: 1% at <0.7, 7% at 0.7–0.8, 28% at 0.8–0.9, 64% at 0.9–1) were used for linkage mapping studies.

Linkage analysis

The genotypic data and map distances were downloaded from the CEPH Version 9 database and the Marshfield map database⁸ using error-checked markers. MERLIN was used to perform nonparametric linkage analysis because it is robust to nonnormal distributions. For quantitative traits, MERLIN uses the following definitions:

$$S(v) = \sum \text{founder alleles } S_{\text{allele}}(v)^2,$$

$$S_{\text{allele}}(v) = \sum \text{all carriers of allele } (y_i - \mu).$$

The score for each inheritance vector $S(v)$ is calculated by summing squared scores for each founder allele. The score for each founder allele is calculated by summing the mean deviates $(y_i - \mu)$ for all individuals who carry the founder allele, in which y_i is the phenotype for individual i , μ is the population mean, and v is the list of individuals who carry a particular founder allele. Inheritance vectors are used to construct a likelihood ratio test for linkage.

Single-nucleotide polymorphisms

From the online CEU dataset in the HapMap project (release 21)⁹, 31,312 high-frequency SNPs covering 1,278 genes within the 1 LOD confidence interval of linkage regions with LOD scores of >1.5 were retrieved. To prevent possible genotyping errors, we excluded the SNPs with Mendelian transmission errors. Remaining SNPs used were those with three genotypes and two counts per genotype in the 60 unrelated parents of the trios.

Association analysis

Eighty-six HapMap CEU samples (of 90) were phenotyped for daunorubicin sensitivity. Three samples (GM11839, GM12716, and GM12717) were not phenotyped due to the inability to grow the cells above 85% viability. Additionally, another sample (GM12236) was not available from Coriell at the time of the experiment. The cytotoxicity values of HapMap CEU cell lines, as part of the CEPH pedigrees, were also transformed using the inverse normalization of the percentile rank function in Microsoft Excel software. Population stratification and total association between the selected 31,312 SNPs and percentage cell survival at 0.0125, 0.025, 0.05, 0.1, 0.2, and 1.0 $\mu\text{mol/L}$ daunorubicin and the IC_{50} was done using the QTDT program. Gender was used as a covariate to adjust for the normalized cytotoxicity values. False discovery rate (FDR) procedure was used to control for multiple testing within each cytotoxic phenotype using R statistics software¹⁰ (25).

Gene ontology classification and pathway analysis

Gene ontology categories and KEGG pathways¹¹ were determined using DAVID¹² (20). DAVID determines overrepresentation by comparing the positive genes to the tested genes in the linkage regions using the one-tailed Fisher exact test.

⁸Marshfield map database; <http://www.research.marshfieldclinic.org/genetics>.

⁹International HapMap Project; <http://www.hapmap.org>.

¹⁰ R statistics software; <http://www.r-project.org>.

¹¹KEGG knowledge database; <http://www.genome.jp/kegg/pathway.html>.

¹²DAVID; <http://niaid.abcc.ncifcrf.gov/>.

Results

Cell cytotoxicity and heritability analysis

Using a short-term cytotoxicity assay, 324 CEPH LCLs derived from 24 three-generation CEPH Utah pedigrees were exposed to increasing concentrations of daunorubicin (0.0125, 0.025, 0.05, 0.1, 0.2, and 1.0 $\mu\text{mol/L}$). These families also contained a subset of 86 HapMap CEU which were used for the association analyses. The mean ($\pm\text{SD}$) percentage of survival decreased from 82.7 ± 13.4 to 11.4 ± 4.8 after 72 h after exposure to 0.0125 to 1 $\mu\text{mol/L}$ daunorubicin (Table 1). The mean and median concentration required to inhibit 50% cell growth (IC_{50}) for these 324 cell lines were 0.051 and 0.046 $\mu\text{mol/L}$, respectively. These values were within the range of the IC_{50} 's determined for a panel of NCI60 human tumor cell lines¹³ treated with daunorubicin (range, 0.003–1.58 $\mu\text{mol/L}$; mean, 0.084 $\mu\text{mol/L}$). The frequency distributions of the percentage cell growth inhibition after daunorubicin treatment for the 324 cell lines are shown in Supplementary Fig. S1. Six phenotypes (percentage cell survival at 0.0125, 0.05, 0.1, 0.2, and 1.0 $\mu\text{mol/L}$ daunorubicin and IC_{50} for 324 LCLs) were not normally distributed ($P < 0.05$) based on Kolmogorov-Smirnov statistic, whereas percentage survival after 0.025 $\mu\text{mol/L}$ daunorubicin treatment was normally distributed. All phenotype data were transformed using the inverse normalization of the percentile rank function in Microsoft Excel software. The variations of the cytotoxic phenotypes within and between 24 CEPH families are illustrated as boxplots and are shown in Fig. 1 and Supplementary Fig. S2. There were significant genetic contributions to all seven cytotoxic phenotypes ($h^2 = 0.18\text{--}0.63$; Table 1). The heritability for the IC_{50} ($0.051 \pm 0.048 \mu\text{mol/L}$) phenotype was 0.29 ($P = 8 \times 10^{-7}$). There were no sex-specific heritability effects for any of the daunorubicin phenotypes (data not shown).

Linkage analysis

Nonparametric linkage analysis was done on seven daunorubicin phenotypes using 7,209 high heterozygous SNPs and microsatellite markers. Drug cytotoxicity is a multigenic trait; therefore, LOD of >1.5 was chosen in an attempt to be inclusive of genes that may contribute to a small extent. The findings from MERLIN multipoint analyses, in which LOD scores exceeded 1.5, are summarized in Table 2. Among the seven phenotypes, there were 11 linkage peaks with a maximum LOD score of larger than 1.5 (Supplementary Fig. S3). The highest LOD score (3.18) that reached genome-wide significance was located on 4q28.2 to 4q32.3 for the 0.05 $\mu\text{mol/L}$ daunorubicin treatment phenotype (Supplementary Fig. S3, peak D and Fig. 2). It is worth noting that this region also contained suggestive LOD scores for other phenotypes corresponding to 0.025, 0.1, and 0.2 $\mu\text{mol/L}$ and IC_{50} daunorubicin phenotypes with LOD scores of 1.72, 2.53, 1.91, and 2.05, respectively (Fig. 2). This implies that the same linkage region confer sensitivity to daunorubicin-induced cytotoxicity in all concentrations except the highest and lowest concentration. Examination of the linkage peaks associated with the lowest daunorubicin treatment concentration revealed a peak with a maximum LOD score of 2.11 at 16q23.1 to 16q24.1 (Supplementary Fig. S3, peak K and Fig. 3), extending from 104 to 118 Mb of chromosome 16. This concentration-dependent phenomenon is further supported by a hierarchical cluster view of the seven daunorubicin phenotypes (Supplementary Fig. S4). Two major distinguishable groups are formed between the two lowest daunorubicin concentrations (0.0125 and 0.025 $\mu\text{mol/L}$) and higher concentrations including IC_{50} . The middle daunorubicin concentrations (IC_{50} , 0.05, 0.1, and 0.2 $\mu\text{mol/L}$) were more closely clustered together within the subgroup. Not surprisingly, unique genes are associated with the lowest concentration of daunorubicin, suggesting that genetic contribution to drug cytotoxicity varies with drug concentration.

¹³NCI60; <http://dtp.nci.nih.gov/>.

Association results

The association studies were done using the percentage survival data from seven daunorubicin phenotypes and 31,312 SNPs in the 1 LOD confidence interval of the 11 linkage regions (Table 2). These SNPs are located throughout 1,278 genes. Using an FDR threshold of 10%, a total of 137 SNPs from 30 genes were shown to be significantly associated with daunorubicin cytotoxic phenotypes ($P \leq 2 \times 10^{-4}$, $FDR \leq 0.1$; see Table 3 and Supplementary Table S1). An intronic SNP (rs978752) of *INPP4B* in the chromosome 4 linkage peak is associated with multiple concentrations of daunorubicin (0.1 $\mu\text{mol/L}$, $P = 2 \times 10^{-4}$, $FDR = 0.1$; 0.2 $\mu\text{mol/L}$, $P = 4 \times 10^{-5}$, $FDR = 0.22$; 1 $\mu\text{mol/L}$, $P = 3 \times 10^{-5}$, $FDR = 0.66$; Fig. 2). The genotype CC of SNP rs978752 (*INPP4B*) is correlated with greater cell sensitivity to 1 $\mu\text{mol/L}$ daunorubicin (Fig. 2) and with other daunorubicin concentrations (0.1 and 0.2 $\mu\text{mol/L}$; Supplementary Table S1). As shown in Fig. 3, multiple intronic SNPs of *CDH13* in the chromosome 16 linkage peak are significantly associated with 0.0125 $\mu\text{mol/L}$ daunorubicin ($P \leq 2 \times 10^{-4}$, $FDR \leq 0.1$). SNP rs1862831 AA genotype is associated with greater cell sensitivity to 0.0125 $\mu\text{mol/L}$ daunorubicin-induced cytotoxicity. The linkage-directed association study in HapMap CEU resulted in significant associations in 9 of 11 linkage regions (Table 3). The two linkage regions that did not result in significant association signals were at 6p12.3 to 6q14 (LOD, 1.58) and 8q24 to 8q24.2 (LOD, 1.68) for 0.05 and 0.0125 $\mu\text{mol/L}$ daunorubicin, respectively.

Pathway analysis

Using 1,278 genes in 1 LOD confidence interval of 11 linkage regions as the background, the 30 genes that were significantly associated with daunorubicin cytotoxic phenotypes were imported for gene ontology and KEGG pathway analysis. The results showed that phosphatidylinositol signaling system ($P = 0.034$; PIK3R1 and *INPP4B*), GPI-anchored proteins ($P = 0.027$; *CDH13*, *GPC5*, and *LSAMP*), and axon guidance pathway ($P = 0.06$; *NGEF* and *SLIT3*) were significantly or marginally overrepresented in the candidate gene list (Table 3).

Discussion

Identification of genetic variants that predict chemotherapeutic outcome is critical for the design of individualized therapy. With enriched publicly available resources of marker genotypes^{9,14,15} and gene transcriptional levels¹⁶, the LCL system has been used in the mapping of genetic variants influencing cell response to IR-induced stress (26), cytotoxicity (21,27), and variation in mRNA expression level (28). In the current study, we found that daunorubicin-induced cytotoxicity is a highly heritable trait, and there are genetic variants associated with this trait. Our approach decreased multiple testing problems inherent with whole-genome association studies by limiting the association studies to genomic regions identified through linkage analysis. Instead of testing 3.2 million SNPs throughout the genome, only 31,312 SNPs representing 1,281 genes within linkage regions ($LOD \geq 1.5$) were tested, with 30 genes showing significant association with cellular susceptibility to daunorubicin.

The present study strongly suggests that sensitivity to daunorubicin-induced cytotoxicity is a polygenic trait with different genes contributing at different concentrations of drug. The fluctuation of estimated heritability values at differing drug concentrations suggests that genetic components contributing to human variation in daunorubicin-induced cytotoxicity are dose dependent. Linkage peaks differing at low versus high drug concentrations further imply that some genes are likely turned on at lower concentrations of drug, whereas others contribute

¹⁴CEPH database; <http://www.cephb.fr/cephdb/>.

¹⁵Perlegen; <http://www.perlegen.com>.

¹⁶Focus array transcriptional levels; <http://www.ncbi.nlm.nih.gov/geo/query/acc.cgi?acc=GSE1485>.

to variation in susceptibility to cytotoxicity at higher dosages. This is in agreement with previous work demonstrating that cell-cycle arrest and cell death follow distinct pathways depending on the daunorubicin concentration (19) and other investigators showing higher daunorubicin doses correlating to more rapid caspase-3 induction (29). Our hierarchical cluster view of the seven daunorubicin phenotypes further support this concept with midrange drug concentration treatment effects clustering together, whereas the percentage cell survival at the highest and lowest concentration exhibit distinguishable patterns.

To date, candidate gene approaches have focused on genes that most likely play a role in the pharmacokinetic and pharmacodynamics of daunorubicin. However, evaluation of a genetic polymorphism within the multidrug resistance 1 gene, whose expression correlated to daunorubicin resistance (30) in acute myeloid leukemia cell lines showed a negative correlation between this polymorphism and response to doxorubicin, an analogue of daunorubicin (31). In addition, association studies conducted for genetic variants located in topoisomerase II, c-raf, bcl-2, and p53, whose expression correlates with resistance to anthracyclines (32), also yielded negative results (33,34). There are several reasons for these discrepancies, including the multigenic nature of sensitivity of cells to drugs and the cell-specific nature of these candidate genes. Our whole-genome approach, which makes no *a priori* assumptions and gives equal weight to all genes, would more likely identify genetic polymorphism signatures that are important to daunorubicin-induced cytotoxicity. These signatures include all SNPs within the 30 genes identified using our linkage-directed association studies.

Dolan et al. (21) and Watters et al. (27) have shown that sensitivity to cytotoxicity induced by cisplatin, 5-fluorouracil, and docetaxel are heritable traits, which might be influenced by many low penetrance genes. The present study differs from these previously published studies in several ways: (a) the present analysis reports heritability, linkage, and association studies of daunorubicin; (b) the power of the linkage scan is enhanced by a significant increase in the sample size (24 pedigrees) and the marker density (7,209 markers), compared with 10 pedigrees and 1,784 markers in our previous study (21); (c) association studies were not done in previous studies, whereas the present analysis includes linkage-directed association studies using trios that are part of the HapMap CEU cell lines, thereby providing dense SNP coverage; (d) pathway and gene ontology analysis was done, showing that genes associated with daunorubicin cytotoxicity were overrepresented in phosphatidylinositol signaling system consistent with literature evidence (35), axon guidance pathway, and GPI-anchored proteins family.

Our linkage-directed association analyses identified 30 genes showing significant association with cellular susceptibility to daunorubicin and located under the linkage peaks. Although all 30 genes are considered equally important, the SNPs located within *PIK3R1* and *INPP4B* and corresponding phosphatidylinositol signaling pathway is of considerable interest. The phosphatidylinositol signaling pathway involves the metabolism of inositol lipids. The lipid products, such as phosphatidylinositol-3,4- biphosphate and phosphatidylinositol-3,4,5-triphosphate, have been shown to interact with a large variety of downstream effectors, including serine-threonine kinase Akt (36). It was observed that daunorubicin could stimulate the phosphoinositide-3 kinase (PI3K)/Akt-mediated survival pathway in human acute myeloid leukemia cell lines (37); and PI3K has been shown to protect cells from another anthracycline, doxorubicin-induced apoptosis (38). *PIK3R1* encodes the 85 kDa regulatory subunit of PI3K, which was reported to be involved in generating the antiapoptotic and chemoresistant phenotype associated with accelerated local tumor recurrence (39). *INPP4B* encoding inositol polyphosphate 4-phosphatase type II is also involved in phosphatidylinositol signaling pathways. Our genetic analysis identifying the phosphatidylinositol signaling pathway, particularly PI3K, is consistent with literature evidence demonstrating that the pathway contributes to protection from daunorubicin-induced cytotoxicity (38).

The utility of daunorubicin is limited by a dose-dependent cardiotoxicity (10) that can lead to long-term side effects and severe morbidity (8). In a study on childhood leukemia, nearly 60% of 115 survivors had echocardiographic abnormalities in heart function (40). Attempts to reduce anthracycline cardiotoxicity have been directed toward dose and schedule modification, developing less cardiotoxic analogues and concurrently administering cardioprotective agents to attenuate the effects of anthracyclines on the heart (41); however, the genetic basis of anthracycline-induced cardiotoxicity is largely unknown. Although our unbiased genetic model uses lymphoblastoid, not cardiac, cells, the ultimate goal is to identify variants that predispose an individual to the toxicities associated with daunorubicin. Of the 30 genes we identified in LCLs, 19 were also expressed in human cardiac tissue as shown in a gene expression study¹⁷ carried out by Shumueli et al. (42). The model provides genetic leads that can be evaluated in the appropriate tissue of toxicity, such as cardiac. Particular genes of interest that are expressed in the heart include *CDH13*, a member of the cadherin superfamily, encoding a putative mediator of cell-cell interaction in the heart, although any of the identified genes or combination of genes could be important.

Although the full implications and biological significance of other genes and networks identified through our approach are not yet completely understood, they may serve as a platform to further explore relevant mechanisms and improve the understanding of the molecular basis of daunorubicin-induced cytotoxicity. Moreover, this study also highlights similarities and differences among seven daunorubicin cytotoxic phenotypes at the molecular level. Because family studies cannot be done in unaffected individuals, human LCLs represent our best *in vitro* model with extensive genotypic information in the public domain. We recognize limitations, such as differences in expression and posttranslational modification of genes in various tissues.

In summary, using heritability analysis and whole-genome linkage scan with linkage-directed association studies, we provide a balanced approach to decipher the genetic factors contributing to chemotherapy-induced cytotoxicity. Our data suggests that genetic factors contribute to cytotoxicity to a greater degree at lower concentrations of daunorubicin indicating the relative contribution of genetic factors and environment may vary depending on the dosage of daunorubicin. Three overrepresented pathways and 30 genes are associated with the daunorubicin-induced cytotoxicity in the linkage-directed association studies. Although the relatively small sample size in the association studies produce results that require confirmation, the findings obtained may be important in relation to the ongoing search for genes responsible for the mechanism of daunorubicin-associated toxicity. Furthermore, this model can be applied to any phenotype that can be evaluated in LCLs.

Supplementary Material

Refer to Web version on PubMed Central for supplementary material.

Acknowledgments

Grant support: NIH/National Institute of General Medical Sciences (NIGMS) grant GM61393 and NIH/NIGMS Pharmacogenetics Research Network and Database, U01GM61374 (Russ Altman, PI; <http://pharmgkb.org>)

References

1. Davis HL, Davis TE. Daunorubicin and Adriamycin in cancer treatment: an analysis of their roles and limitations. *Cancer treatment reports* 1979;63:809–815. [PubMed: 378369]

¹⁷GeneCards; <http://www.genecards.org>.

2. Chaires JB, Fox KR, Herrera JE, Britt M, Waring MJ. Site and sequence specificity of the daunomycin-DNA interaction. *Biochemistry* 1987;26:8227–8236. [PubMed: 2831939]
3. Bachur NR, Yu F, Johnson R, Hickey R, Wu Y, Malkas L. Helicase inhibition by anthracycline anticancer agents. *Mol Pharmacol* 1992;41:993–998. [PubMed: 1614415]
4. Palayoor ST, Stein JM, Hait WN. Inhibition of protein kinase C by antineoplastic agents: implications for drug resistance. *Biochem Biophys Res Commun* 1987;148:718–725. [PubMed: 3689368]
5. Ohmori T, Podack ER, Nishio K, et al. Apoptosis of lung cancer cells caused by some anti-cancer agents (MMC, CPT-11, ADM) is inhibited by bcl-2. *Biochem Biophys Res Commun* 1993;192:30–36. [PubMed: 8476431]
6. Seiter K. Toxicity of the topoisomerase II inhibitors. *Expert Opin Drug Saf* 2005;4:219–234. [PubMed: 15794715]
7. Young RC, Ozols RF, Myers CE. The anthracycline antineoplastic drugs. *N Engl J Med* 1981;305:139–153. [PubMed: 7017406]
8. Lipshultz SE. Exposure to anthracyclines during childhood causes cardiac injury. *Semin Oncol* 2006;33:S8–S14. [PubMed: 16781284]
9. Elliott P. Pathogenesis of cardiotoxicity induced by anthracyclines. *Semin Oncol* 2006;33:S2–S7. [PubMed: 16781283]
10. Wouters KA, Kremer LC, Miller TL, Herman EH, Lipshultz SE. Protecting against anthracycline-induced myocardial damage: a review of the most promising strategies. *Br J Haematol* 2005;131:561–578. [PubMed: 16351632]
11. Chen QM, Alexander D, Sun H, et al. Corticosteroids inhibit cell death induced by doxorubicin in cardiomyocytes: induction of antiapoptosis, antioxidant, and detoxification genes. *Mol Pharmacol* 2005;67:1861–1873. [PubMed: 15755911]
12. Yi X, Bekeredjian R, DeFilippis NJ, Siddiquee Z, Fernandez E, Shohet RV. Transcription analysis of doxorubicin-induced cardiotoxicity. *Am J Physiol* 2006;290:H1098–H1102.
13. Kizaki K, Ito R, Okada M, et al. Enhanced gene expression of myocardial matrix metalloproteinases 2 and 9 after acute treatment with doxorubicin in mice. *Pharmacol Res* 2006;53:341–346. [PubMed: 16455267]
14. Cao W, Ma SL, Tang J, Shi J, Lu Y. A combined treatment TNF- α /doxorubicin alleviates the resistance of MCF-7/Adr cells to cytotoxic treatment. *Biochim Biophys Acta* 2006;1763:182–187. [PubMed: 16483679]
15. Gruber A, Briese B, Arestrom I, Vitols S, Bjorkholm M, Peterson C. Effect of verapamil on daunorubicin accumulation in human leukemic cells with different levels of MDR1 gene expression. *Leuk Res* 1993;17:353–358. [PubMed: 8487584]
16. Boland MP, Foster SJ, O’Neill LA. Daunorubicin activates NF κ B and induces κ B-dependent gene expression in HL-60 promyelocytic and Jurkat T lymphoma cells. *J Biol Chem* 1997;272:12952–12960. [PubMed: 9148901]
17. Yasui K, Wakabayashi I, Negoro M, Suehiro A, Kakishita E. Daunorubicin inhibits gene expression of cyclooxygenase-2 in vascular smooth muscle cells. *Thromb Res* 2001;103:233–240. [PubMed: 11672585]
18. Gupta M, Kumar A, Dabadghao S. Resistance of bcrabl-positive acute lymphoblastic leukemia to daunorubicin is not mediated by mdr1 gene expression. *Am J Hematol* 2002;71:172–176. [PubMed: 12410571]
19. Mansilla S, Pina B, Portugal J. Daunorubicin-induced variations in gene transcription: commitment to proliferation arrest, senescence and apoptosis. *Biochem J* 2003;372:703–711. [PubMed: 12656675]
20. Almasy L, Blangero J. Multipoint quantitative-trait linkage analysis in general pedigrees. *Am J Hum Genet* 1998;62:1198–1211. [PubMed: 9545414]
21. Dolan ME, Newbold KG, Nagasubramanian R, et al. Heritability and linkage analysis of sensitivity to cisplatin-induced cytotoxicity. *Cancer Res* 2004;64:4353–4356. [PubMed: 15205351]
22. O’Connell JR, Weeks DE. PedCheck: a program for identification of genotype incompatibilities in linkage analysis. *Am J Hum Genet* 1998;63:259–266. [PubMed: 9634505]
23. Sun L, Wilder K, McPeck MS. Enhanced pedigree error detection. *Hum Hered* 2002;54:99–110. [PubMed: 12566741]

24. Abecasis GR, Cherny SS, Cookson WO, Cardon LR. Merlin-rapid analysis of dense genetic maps using sparse gene flow trees. *Nat Genet* 2002;30:97–101. [PubMed: 11731797]
25. Benjamini Y, Yekutieli D. Quantitative trait Loci analysis using the false discovery rate. *Genetics* 2005;171:783–790. [PubMed: 15956674]
26. Jen KY, Cheung VG. Transcriptional response of lymphoblastoid cells to ionizing radiation. *Genome Res* 2003;13:2092–2100. [PubMed: 12915489]
27. Watters JW, Kraja A, Meucci MA, Province MA, McLeod HL. Genome-wide discovery of loci influencing chemotherapy cytotoxicity. *Proc Natl Acad Sci U S A* 2004;101:11809–11814. [PubMed: 15282376]
28. Morley M, Molony CM, Weber TM, et al. Genetic analysis of genome-wide variation in human gene expression. *Nature* 2004;430:743–747. [PubMed: 15269782]
29. Masquelier M, Zhou QF, Gruber A, Vitols S. Relationship between daunorubicin concentration and apoptosis induction in leukemic cells. *Biochem Pharmacol* 2004;67:1047–1056. [PubMed: 15006541]
30. Johnsson A, Vallon-Christensson J, Strand C, Litman T, Eriksen J. Gene expression profiling in chemoresistant variants of three cell lines of different origin. *Anticancer Res* 2005;25:2661–2668. [PubMed: 16080509]
31. Efferth T, Sauerbrey A, Steinbach D, et al. Analysis of single nucleotide polymorphism C3435T of the multi-drug resistance gene MDR1 in acute lymphoblastic leukemia. *Int J Oncol* 2003;23:509–517. [PubMed: 12851703]
32. Cioca DP, Aoki Y, Kiyosawa K. RNA interference is a functional pathway with therapeutic potential in human myeloid leukemia cell lines. *Cancer Gene Ther* 2003;10:125–133. [PubMed: 12536201]
33. Scheltema JM, Romijn JC, van Steenbrugge GJ, Beck WT, Schroder FH, Mickisch GH. Decreased levels of topoisomerase II α in human renal cell carcinoma lines resistant to etoposide. *J Cancer Res Clin Oncol* 1997;123:546–554. [PubMed: 9393588]
34. Sturm I, Bosanquet AG, Hummel M, Dorken B, Daniel PT. In B-CLL, the codon 72 polymorphic variants of p53 are not related to drug resistance and disease prognosis [electronic resource]. *BMC Cancer* 2005;5:105. [PubMed: 16109171]
35. Laurent G, Jaffrezou JP. Signaling pathways activated by daunorubicin. *Blood* 2001;98:913–924. [PubMed: 11493433]
36. Franke TF, Kaplan DR, Cantley LC. PI3K: down-stream AKTion blocks apoptosis. *Cell* 1997;88:435–437. [PubMed: 9038334]
37. Plo I, Bettaieb A, Payrastra B, et al. The phosphoinositide 3-kinase/Akt pathway is activated by daunorubicin in human acute myeloid leukemia cell lines. *FEBS Lett* 1999;452:150–154. [PubMed: 10386580]
38. O’Gorman DM, McKenna SL, McGahon AJ, Knox KA, Cotter TG. Sensitisation of HL60 human leukaemic cells to cytotoxic drug-induced apoptosis by inhibition of PI3-kinase survival signals. *Leukemia* 2000;14:602–611. [PubMed: 10764145]
39. Coffey JC, Wang JH, Smith MJ, et al. Phosphoinositide 3-kinase accelerates postoperative tumor growth by inhibiting apoptosis and enhancing resistance to chemotherapy-induced apoptosis. Novel role for an old enemy. *J Biol Chem* 2005;280:20968–20977. [PubMed: 15741161]
40. Lipshultz SE, Colan SD, Gelber RD, Perez-Atayde AR, Sallan SE, Sanders SP. Late cardiac effects of doxorubicin therapy for acute lymphoblastic leukemia in childhood. *N Engl J Med* 1991;324:808–815. [PubMed: 1997853]
41. Iarussi D, Indolfi P, Casale F, Martino V, Di Tullio MT, Calabro R. Anthracycline-induced cardiotoxicity in children with cancer: strategies for prevention and management. *Paediatr Drugs* 2005;7:67–76. [PubMed: 15871628]
42. Shmueli O, Horn-Saban S, Chalifa-Caspi V, et al. GeneNote: whole genome expression profiles in normal human tissues. *C R Bio* 2003;326:1067–1072. [PubMed: 14744114]

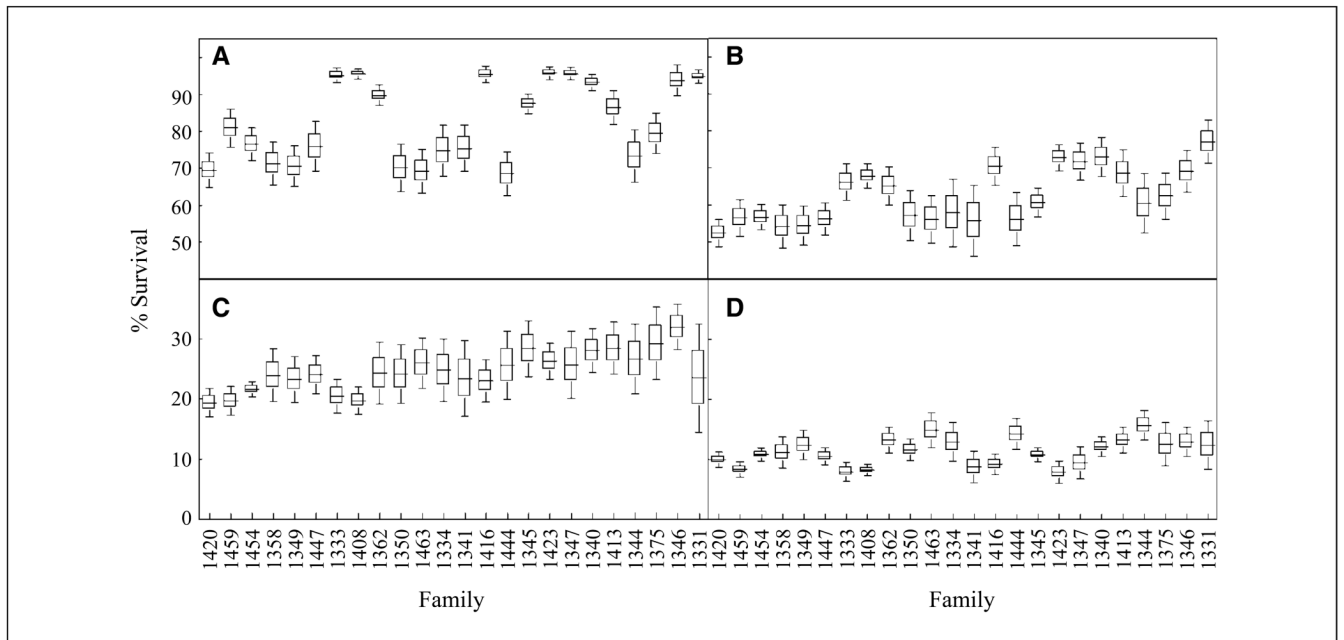


Figure 1.

Boxplots for 324 cell lines within 24 pedigrees are shown for various concentrations of daunorubicin, illustrating interfamily and intrafamily variance. The mean for each family's percentage survival after daunorubicin treatment for 72 h with (A) 0.0125 $\mu\text{mol/L}$; (B) 0.025 $\mu\text{mol/L}$; (C) 0.2 $\mu\text{mol/L}$, and (D) 1.0 $\mu\text{mol/L}$. *Line*, mean phenotypic response within each family; *box*, mean \pm SE; *whiskers*, mean $\pm 1.97 \times$ SE.

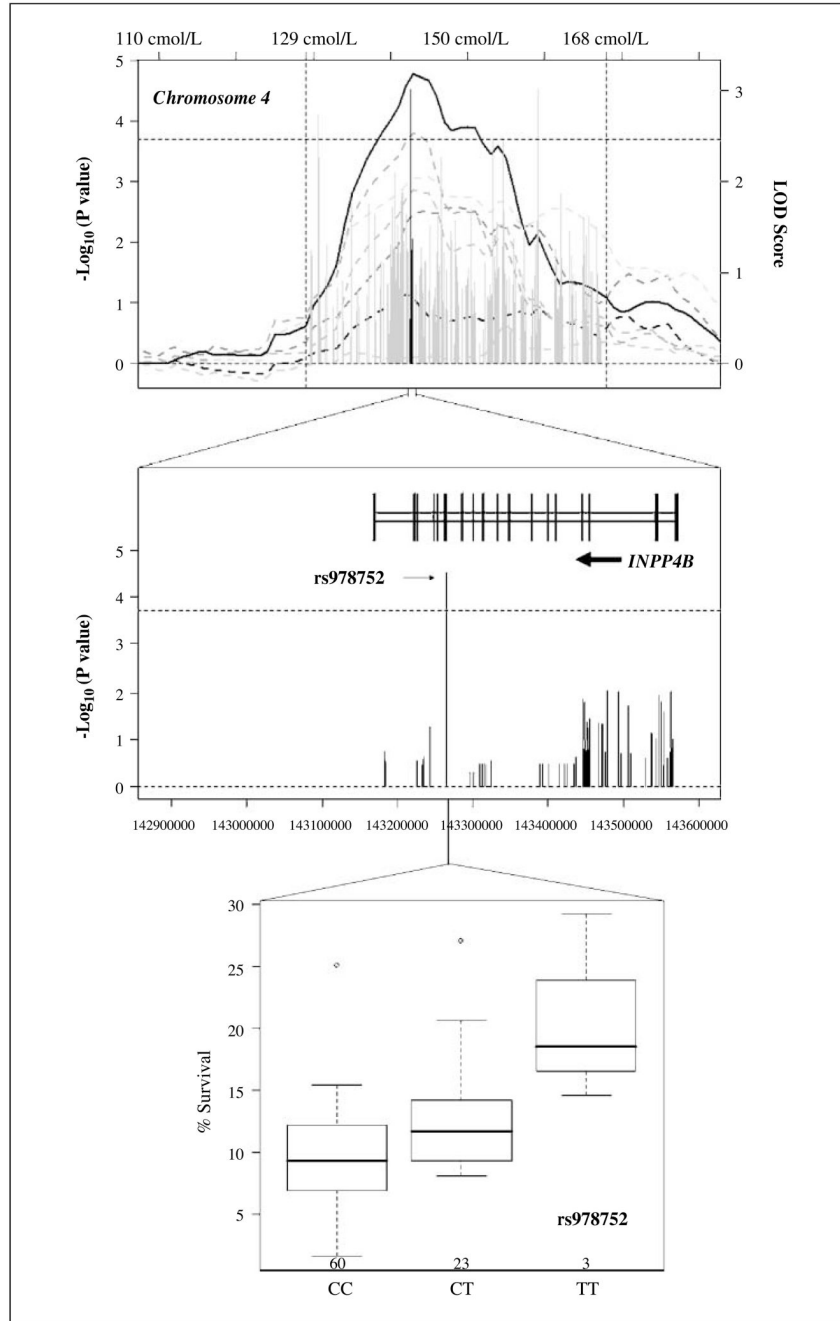


Figure 2. Linkage-directed association studies on chromosome 4 to identify SNPs conferring sensitivity to daunorubicin-induced cytotoxicity. *Top*, results from linkage analysis based on 24 CEPH families. The 1 LOD confidence interval of the peak on chromosome 4 from multipoint linkage of daunorubicin-induced cytotoxicity (0.05 $\mu\text{mol/L}$: *black solid curve*) and from the linkage analysis of 0.1 $\mu\text{mol/L}$, IC_{50} , 0.2 $\mu\text{mol/L}$, 0.025 $\mu\text{mol/L}$, and 0.0125 $\mu\text{mol/L}$ (*dotted curves with peaks in descending order*). *Vertical dashed lines*, 1 LOD confidence interval of the linkage peaks for the follow-up association studies; *horizontal dashed lines*, P value of 2×10^{-4} . Results of QTDT analysis using genotypes for 30 CEU trios from the HapMap Project (*gray bars*) and associated genotypes within *INPP4B* (*black bars*). *Middle*, results of QTDT

analysis illustrating associated genotypes within *INPP4B*. *Bottom*, SNP (rs978752) located in the 16th intron of *INPP4B* gene shows suggestive association evidence with daunorubicin (1 $\mu\text{mol/L}$)–induced cytotoxicity (FDR = 0.66, $P = 3 \times 10^{-5}$). This SNP is also modestly associated with other daunorubicin phenotypes (0.1 $\mu\text{mol/L}$: FDR = 0.1, $P = 2 \times 10^{-4}$; 0.2 $\mu\text{mol/L}$: FDR = 0.22, $P = 4 \times 10^{-5}$).

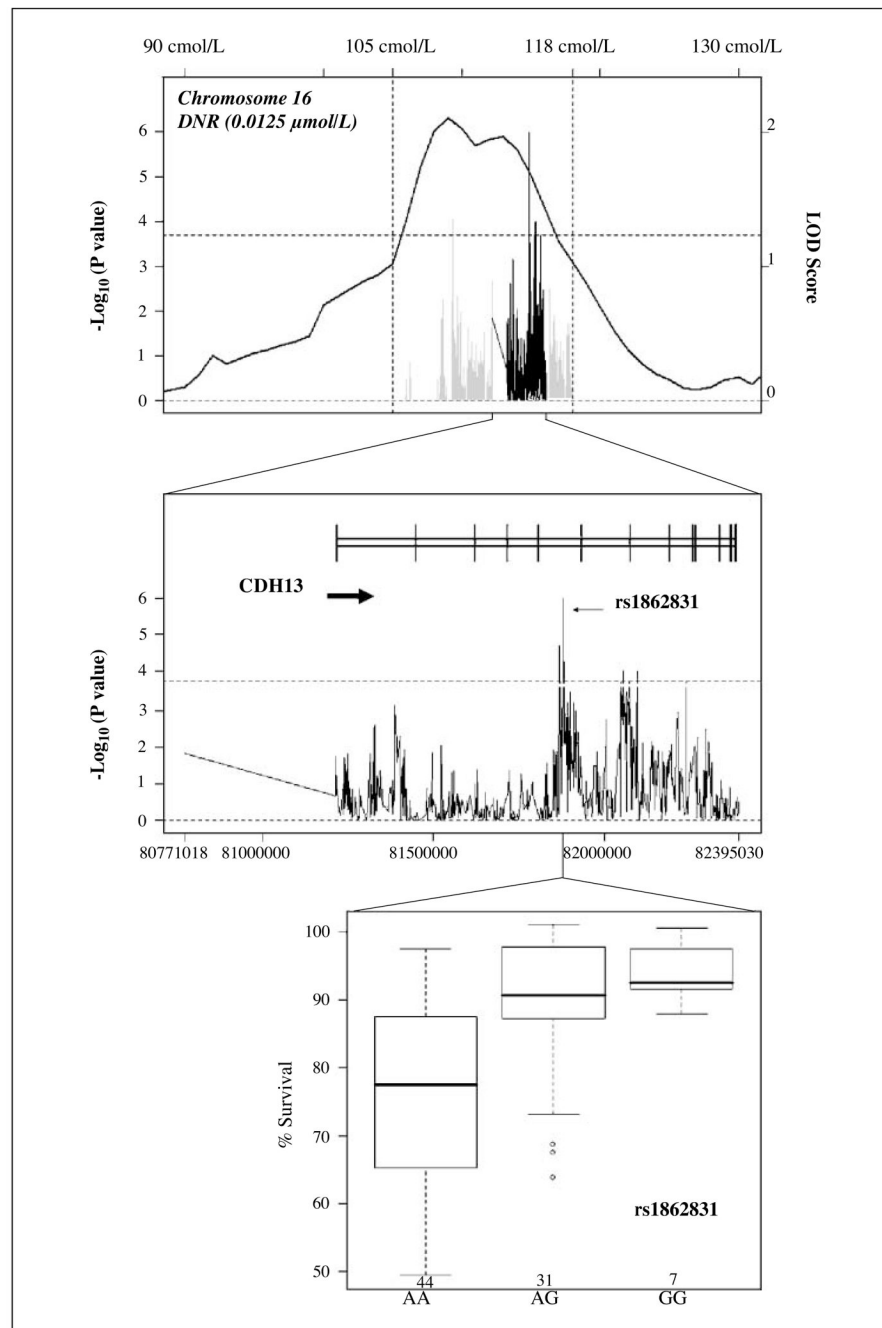


Figure 3. Linkage-directed association studies on chromosome 16 to identify SNPs conferring sensitivity to daunorubicin-induced cytotoxicity. *Top*, results from linkage analysis based on 24 CEPH families. The 1 LOD confidence interval of the peak on chromosome 16 from multipoint (*solid curve*) linkage of daunorubicin (0.0125 $\mu\text{mol/L}$)–induced cytotoxicity. *Vertical dashed lines*, 1 LOD confidence interval of the linkage peaks for the follow-up association studies; *horizontal dashed lines*, P value of 2×10^{-4} . Results of QTDT analysis using genotypes for 30 CEU trios from the HapMap Project (*gray bars*) and associated genotypes within *CDH13* (*black bars*). *Middle*, results of QTDT analysis illustrating associated genotypes within

CDH13. Bottom, SNP rs1862831 in the fifth intron of *CDH13* gene are associated with daunorubicin (0.0125 $\mu\text{mol/L}$)–induced cytotoxicity (FDR = 0.03, $P = 1 \times 10^{-6}$).

Table 1

Cell survival and heritability after different concentrations of daunorubicin for 72-h treatment in 24 CEPH pedigrees

Drug concentration ($\mu\text{mol/L}$)	Mean percentage survival in CEPH pedigrees (mean percentage survival in HapMap CEU trios)*	Heritability (h^2)	<i>P</i> value for h^2
0.0125	82.7 \pm 13.4 (82.4 \pm 13.7)	0.63	$<1.0 \times 10^{-7}$
0.025	62.6 \pm 12.8 (62.3 \pm 13.2)	0.41	$<1.0 \times 10^{-7}$
0.05	45.3 \pm 10.8 (45.3 \pm 11.7)	0.18	3.6×10^{-3}
0.1	34.3 \pm 10.1 (33.8 \pm 10.6)	0.19	1.7×10^{-3}
0.2	24.6 \pm 9.1 (23.9 \pm 9.2)	0.18	2.1×10^{-3}
1	11.4 \pm 4.8 (10.9 \pm 4.8)	0.33	$<1.0 \times 10^{-7}$

* Data are presented as mean \pm SD from either 324 LCLs in 24 three-generation CEPH families or 30 HapMap CEU trios.

Table 2
Linkage analysis results summarizing peaks with LOD >1.5

Peak*	1 LOD confidence interval	Maximum LOD	Retrieved HapMap SNPs †	Number of genes covered by SNPs	Doxorubicin concentration (μmol/L)
A	1q31–32	1.81	2842	183	1
B	2q36.3–37.3	1.8	2719	140	0.025
C	3q13.12–21.2	1.78	3795	146	1
D	4q28.2–32.3	1.72	3067	174	0.025
		3.18	3067	174	0.05
		2.53	3067	174	0.1
		1.91	3067	174	0.2
		2.05	3067	174	IC ₅₀
E	5p13.1–5q13.3	1.87	3905	173	0.05
F	5q34–35.2	1.57	2370	88	0.025
		1.62	2370	88	0.1
G	6p12.3–6q14	1.58	4121	159	0.05
H	8q24–24.2	1.68	1931	45	0.0125
I	11p14.3–13	1.71	2449	102	0.1
J	13q31.3–32	1.72	2209	38	0.1
		1.85	2209	38	0.2
K	16q23.1–24.1	2.11	1901	33	0.0125

NOTE: LOD score of >1.5 was considered as supportive evidence of linkage.

* Letter corresponds to peak labeled on Supplemental Fig. S3.

† Genotypes are retrieved from HapMap CEU genotype database. All SNPs meet the requirements of no Mendelian errors, three genotypes, and two counts per genotype in the 60 unrelated parents of the HapMap trios.

Table 3
Known and unknown genes derived from significant linkage peak regions and also significantly associated with daunorubicin cytotoxicity

Gene symbol	Cytoband	Description	0.0125 μmol/L	0.025 μmol/L	0.05 μmol/L	0.1 μmol/L	0.2 μmol/L	1 μmol/L	IC ₅₀	Functional pathway or categories or evidence
<i>CACNA1S</i>	1q32	Calcium channel, voltage-dependent, L type, α1S subunit	++							Cardiovascular disease
<i>SKIP</i> †	2q36	Sphingosine kinase type 1 interacting protein		++	+				++	Regulation of cell proliferation
<i>LOC646794</i>	2q36.3	Similar to EAP30 subunit of ELL complex	++							Unknown
<i>TM4SF20</i> †	2q36.3	Transmembrane 4 L six family member 20			+	++	+		++	Integral to membrane
<i>NGEF</i> †	2q37	Neuronal guanine nucleotide exchange factor		++	+					Axon guidance
<i>SP110</i> †	2q37.1	SP110 nuclear body protein				++	+			Pulmonary tuberculosis
<i>ILKAP</i> †	2q37.3	Integrin-linked kinase-associated serine/threonine phosphatase 2C		++						Cell cycle
<i>KIF1A</i> †	2q37.3	Kinesin family member 1A				++				Membrane transport
<i>TAGLN3</i> †	3q13.2	Transgelin 3							++	Central nervous system development
<i>ZBTB20</i> †	3q13.2	Zinc finger and BTB domain containing 20	++							DNA binding
<i>LSAMP</i> †	3q13.2-q21	Limbic system-associated membrane protein				++				GPI anchor
<i>LOC653584</i>	3q13.31	Similar to zinc finger and BTB domain containing 20	++							Unknown
<i>LOC391698</i>	4q28.2	Similar to elongation factor 1-γ (EF-1γ; eEF-1B γ)		++						Unknown
<i>INPP4B</i> †	4q31.21	Inositol polyphosphate-4-phosphatase, type II, 105 kDa				++	+	+		Phosphatidylinositol signaling system
<i>LOC338095</i>	4q32	Proteasome activator subunit 2 pseudogene							++	Unknown
<i>FLJ25371</i>	4q32.1	Hypothetical protein FLJ25371							++	Unknown
<i>FLJ33641</i>	5q11.2	Hypothetical protein FLJ33641			+				++	Unknown
<i>LOC441074</i>	5q11.2	Hypothetical LOC441074	++							Unknown
<i>SDCCAG10</i> †	5q12.3	Serologically defined colon cancer antigen 10			+	++	+		++	Protein folding
<i>MAP1B</i> †	5q13	Microtubule-associated protein 1B				++				Neuronal survival
<i>PIK3R1</i> †	5q13.1	PI3K, regulatory subunit 1 (p85 α)	++							Phosphatidylinositol signaling system

Gene symbol	Cytoband	Description	0.0125 $\mu\text{mol/L}$	0.025 $\mu\text{mol/L}$	0.05 $\mu\text{mol/L}$	0.1 $\mu\text{mol/L}$	0.2 $\mu\text{mol/L}$	1 $\mu\text{mol/L}$	IC ₅₀	Functional pathway or categories or evidence*
<i>RANBP17</i> [†]	5q34	RAN binding protein 17	++							Nuclear export
<i>SLIT3</i>	5q35	Slit homologue 3 (Drosophila)				++	+		++	Axon guidance
<i>TMEM16C</i>	11p14.2	Transmembrane protein 16C				++			++	Integral to membrane
<i>LUZP2</i> [†]	11p14.3	Leucine zipper protein 2	++							Unknown
<i>CLYBL</i> [†]	13q32	Citrate lyase β like	++							Up-regulation of Clybl in murine metastatic tumor cells
<i>GPC5</i>	13q32	Glypican 5				++	+			GPI anchor
<i>CMIP</i> [†]	16q23	c-Maf-inducing protein				++			++	Cellular growth and proliferation
<i>DC13</i> [†]	16q23.2	Chromosome 16 open reading frame 61	++							Unknown
<i>CDH13</i> [†]	16q24.2-q24.3	Cadherin 13, H-cadherin (heart)	++							GPI anchor

NOTE: ++, $\text{FDR} \leq 0.1$ and $\text{P} \leq 2 \times 10^{-4}$; +, $\text{FDR} > 0.1$ and $\text{P} \leq 2 \times 10^{-4}$.

* Pathway, category, and evidence information gathered from KEGG knowledge database and National Center for Biotechnology Information dbGENE. Bold text represents significantly overrepresented pathway.

[†] Gene is expressed in human cardiac tissue as measured by HG-U95A array (42).